Chemical Papers
https://doi.org/10.1007/s11696-019-00738-5

ORIGINAL PAPER

A new Keggin-type heteropolyoxometalates compound built up by coordinated cadmium

Hang Xiao[1] · Xiao-Yuan Wu[2] · Ming-Xue Yang[2] · Lang Lin[1] · Shuai Li[1] · Xin-Yuan Chen[1] · Xiao-Yu Jiang[1]

Received: 4 December 2018 / Accepted: 5 March 2019
© Institute of Chemistry, Slovak Academy of Sciences 2019

Abstract

A new Keggin-type heteropolyoxometalates compound, $\{[Cd(DMA)_4]_2(bibp)(SiW_{12}O_{40})\}_n$ (**1**), (DMA = N, N-dimethylacetamide, bibp = 4,4′-bis(1-imidazolyl) biphenyl) has been synthesized and characterized by single-crystal X-ray diffraction, IR spectrum, elemental analysis, powder X-ray diffraction, thermogravimetric (TG) analysis and electrochemical analysis. Compound **1** is crystallized in orthorhombic with *P*bca space group. The $[SiW_{12}O_{40}]^{4-}$ anions and bibp ligands are linked by coordinated Cd^{2+} ions alternately into a zigzag-like chain, and the chains are extended into a three-dimensional (3D) framework by the C–H···O hydrogen bonds. The cyclic voltammetry analyses show that compound **1** presences of W-centered reversible redox processes and that **1** has electrocatalytic activities towards the reduction of nitrite.

Keywords Heteropolyoxometalate · Coordinated cadmium · Crystal structure · Hydrogen bonds · Electrochemical behavior

Introduction

Polyoxometalates (POMs) have been of interest to researchers, due to the excellent performance of POMs in industrial catalysis, such as rich composition, structural diversity, electronic versatility and its amphoteric (acidic and oxidative) (Zhao et al. 2014, 2016; Jiang et al. 2011). POMs are clusters of early transition metal oxyanions and usually classified into isopolyoxometalates or heteropolyoxometalates, by whether or not heteroatoms (P, Si, etc.) in the composition. The structure of a POM can be adjusted at the molecular level, which can lead to the development of unique electronic properties. One of the most critical features of POMs is the ability to accept or to release a specific number of electrons reversibly, making POMs used as catalysts in the field of electrochemical and electrocatalysis (Wu et al. 2017; Silva and Oliveira 2018; Hu et al. 2017). The rigid organic ligands containing N-donors are used in the construction of compounds with new structures to create unique electrochemical properties (Enferadi-Kerenkan et al. 2018; Proust et al. 2008). In recent years, 4,4′-bis(1-imidazolyl) biphenyl (bibp) as a rigid organic ligand containing N-donors, is widely used for the field of coordination polymers (CPs), metal–organic frameworks (MOFs) (Meng et al. 2017; Zhang et al. 2013). However, there are only a few researches focusing on bibp-based POMs materials.

Herein, we report a new Keggin-type heteropolyoxometalates compound, $\{[Cd(DMA)_4]_2(bibp)(SiW_{12}O_{40})\}_n$ (**1**), in which the bibp units and $[SiW_{12}O_{40}]^{4-}$ anions are linked by coordinated Cd^{2+} ions alternately into a zigzag-like chain. The chains are extended into a three-dimensional (3D) framework by the hydrogen bonds. The electrochemical characterizations of **1** are explored, and its electrocatalytic activity towards the reduction of nitrite is characterized by cyclic voltammetry method.

Electronic supplementary material The online version of this article (https://doi.org/10.1007/s11696-019-00738-5) contains supplementary material, which is available to authorized users.

✉ Xiao-Yu Jiang
xyjiang@fjut.edu.cn

[1] College of the Ecology and Environment Engineering, Fujian University of Technology, Fuzhou 350108, Fujian, China

[2] CAS Key Laboratory of Design and Assembly of Functional Nanostructures, and Fujian Key Laboratory of Nanomaterials, Fujian Institute of Research on the Structure of Matter, Chinese Academy of Sciences, Fuzhou 350002, Fujian, China

Published online: 08 May 2019

Experimental

All the starting chemicals and solvents were purchased commercially from Sinopharm (China) and used without further purification. Pure water was obtained by passing water through a Merck Millipore Direct-Q5UV water purification set (France). The bibp ligand was prepared according to literature (Fan and Hanson 2005). The C, H, O and N elemental analyses were measured on a Vario MICRO elemental analyzer (Germany). The 1H NMR spectra were recorded on a Bruker Avance III 400 MHz NMR spectrometer. X-ray powder diffraction data were recorded on a Mini Flex II diffractometer (China) with a scan speed of 2° min^{-1}. The FT-IR spectra were recorded on a Vertex 70 FT-IR spectrometer (Germany) using KBr pellets in the range of 4000–400 cm^{-1}. Thermogravimetric analyses were carried out on a TGA/DSC1/1100 thermogravimetric analyzer (Switzerland) under a nitrogen atmosphere from 30 to 1000 °C at a heating rate of 15 °C min^{-1}. The electrochemical set-up was a CHI760C electrochemical workstation (China). A conventional three-electrode system was used. The working electrode was a modified glassy carbon electrode (GC). A platinum electrode was used as a counter electrode, and a saturated calomel electrode (SCE) was used as reference electrode. All potentials were measured and reported versus the SCE. All voltammetric experiments were carried out at room temperature.

Synthesis of ligand bibp

A mixture of imidazole (5.76 g, 84 mmol), 4,4′- dibromobiphenyl (6.24 g, 20 mmol), $CuSO_4$ (0.064 g, 0.4 mmol) and K_2CO_3 (8.78 g, 63 mmol) were heated at 180 °C for 12 h, under an argon atmosphere, and then it was gradually cooled to room temperature, washed with water and extracted by ethanol three times. The product was separated and evaporated to dryness to give a solid crude product, which was purified by recrystallization to give a white powder (bibp). Yield: 72%. ^{1}H NMR (400 MHz, $CDCl_3$): δ 7.28 (2H, s), 7.37 (2H, s), 7.53 (4H, d), 7.74 (4H, d), 7.95 (2H, s).

Synthesis of $\{[Cd(DMA)_4]_2(bibp)(SiW_{12}O_{40})\}_n$ (1)

The yellow crystalline compound **1** was prepared via a solvothermal procedure by heat-sealing all reactants into a Teflon-lined stainless container, in weighed amounts of $H_4[SiW_{12}O_{40}]\cdot xH_2O$ (0.1001 g, 0.035 mmol), bibp (0.0102 g, 0.035 mmol), $Cd(NO_3)_2\cdot 4H_2O$ (0.0101 g, 0.035 mmol), 5-aminoisophthalic acid (0.0630 g, 0.035 mmol) and DMA (5.0 mL). The container was heated at 130 °C for 3 days and then cooled to room temperature within 1 day to give yellow block-shaped crystals. The crystals were collected and washed with ethanol. Yield 75% based on Cd. Anal. Calcd. for **1** (%): C, 14.71; H, 2.01; O, 18.82; N, 4.12. Found (%): C, 15.54; H, 1.85; O, 18.25; N, 4.87. FT-IR (KBr pellet, cm^{-1}): 3126w, 2937w, 1601 m, 1514 m, 1402w, 1309w, 1261w, 1192w, 1124w, 1066 m, 1014 m, 972 s, 920 s, 798 s, 530w.

The crystallographic measurement for **1** was taken on a Super Nova CCD diffractometer equipped with a graphite-monochromatic Cu Kα radiation ($\lambda = 1.54178$ Å) at 100 K. Empirical absorption corrections were applied to the data using the CrysAlisPro program (Flack and Bernardinelli 2000). The structure was solved by direct methods using SHELXS-97 and refined with full-matrix least-squares on F^2 using SHELXL-97 program (Sheldrick 2015). All of the non-hydrogen atoms were refined anisotropically. The crystal data of X-ray structural analyses are given in Table S1, and the CCDC reference number is 1855374.

Results and discussion

Single-crystal X-ray structural analysis revealed that compound **1** crystallizes in a centrosymmetric *P*bca space group. Compound **1** is composed of bibp units, $[SiW_{12}O_{40}]^{4-}$ anions, coordinated Cd^{2+} ions, and DMA molecules (Fig. 1). The $[SiW_{12}O_{40}]^{4-}$ anion is in well-known Keggin-type structure, and the central SiO_4 tetrahedron is orientationally disordered where the Si atom is surrounded by eight oxygen atoms, with each oxygen site half-occupied (Shi et al. 2013; Kong et al. 2012). The Si–O bonds range from 1.5883 (210) to 1.7356 (197) Å. W–O bond distances can be divided into three groups: W–O_t (terminal O) 1.6341 (121)–1.6883 (143), W–O_a (O in the SiO_4 tetrahedron) 2.3116 (197)–2.5054 (217) and W–O_b (bridge O) 1.8480 (127)–2.0985 (218) Å, respectively. All coordinated W atoms in **1** are W^{VI} according to BVS calculations (Brese and O'keeffe 1991). The bibp unit is composed of two benzenes and two imidazoles. The two benzenes are on a plane and the two imidazoles on another plane. The angle between the benzene plane and imidazole plane was 38.8°. The Cd^{2+} ion has six-coordination with five oxygen and one nitrogen atoms, four oxygen atoms (O (21), O (22), O (23) and O (24)) from DMA molecule, one (O (1)) from $[SiW_{12}O_{40}]^{4-}$ anion and one nitrogen atom (N (1)) from bibp ligand. Cd–O bonds range are 2.2016 (142)–2.3957 (135) Å, and the Cd–N bond is 2.2062 (162) Å.

$[SiW_{12}O_{40}]^{4-}$ anions and bibp ligands are linked by Cd^{2+} ions alternately into a zigzag-like chain elongation along the *a* axis (Fig. 2). To be viewed in *ab* plane, adjacent chains are connected with the hydrogen bonds C (5)–H (5) ···O (15) to spread out in the *ab* plane (Fig. 3a). Finally, the neighboring planes are balanced to form a 3D

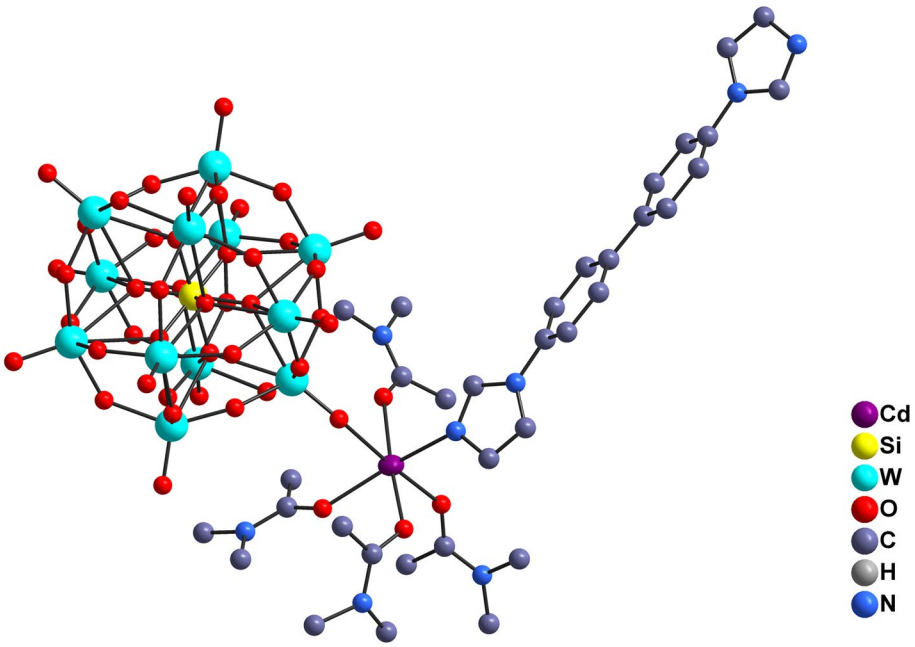

Fig. 1 Ball/stick view of compound **1** (all hydrogen atoms were omitted for clarity)

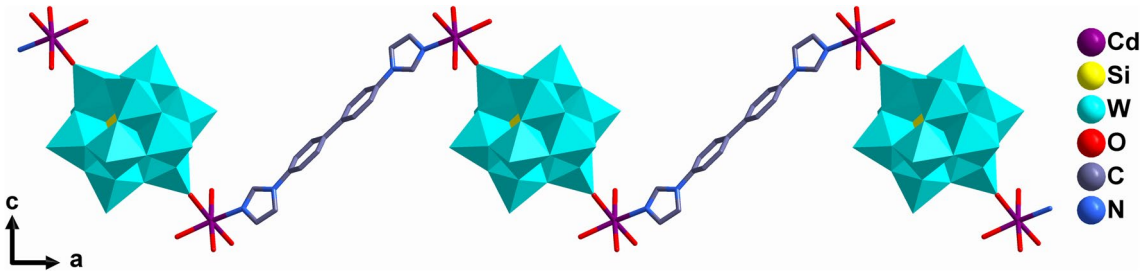

Fig. 2 The zigzag-like chain in compound **1** viewed along the *b* axis

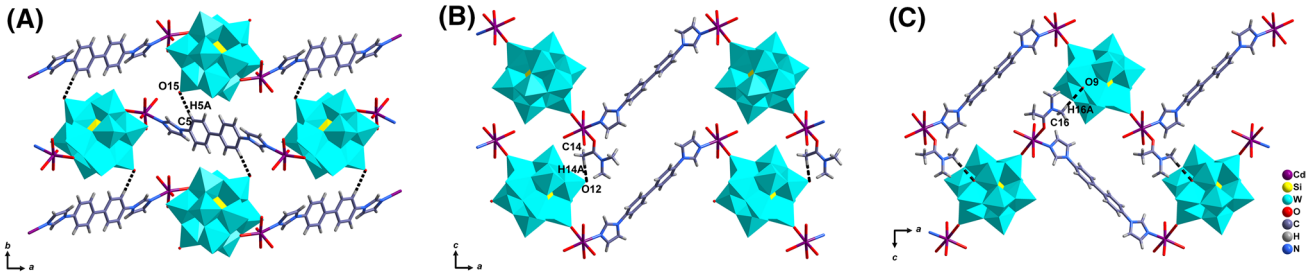

Fig. 3 Three types of hydrogen bonds in compound **1**

supermolecular with hydrogen bonds (C (14)–H (14A) ···O (12) (Fig. 3b) and C (16)–H (16A)···O (9) (Fig. 3c). The C (14)–H (14A) ···O (12) and C (16)–H (16A) ···O (9) involves coordinated DMA molecule and oxygen atoms of polyoxometalate unit, with the D···A distance from 3.4165(322) Å to 3.4853(286) Å and D–H···A angle from 150.0° to 165.8°. C (5)–H (5) ···O (15) involves coordinated bibp ligand and oxygen atoms of polyoxometalate unit, of which the hydrogen bonding parameters (Table S2) (C···O, 3.2357(270) Å, and ∠C–H···O, 154.8°) are in the acceptance range of C–H···O interaction.

In the IR spectrum of **1** (Fig. S1), the vibrations at 1014, 972, 920, 798 cm^{-1} are the characteristic bands of the Keggin-type heteropolyoxometalates, while the vibrations in the region of 3150–1050 cm^{-1} can be attributed to the characteristic peaks of the bibp ligands and the DMA

molecules. In addition, the broad peak at about 3300 cm^{-1} shows the hydrogen bonding interactions in the compound **1**.

The result of the thermogravimetric analysis (TGA) is depicted in Fig. S2. A gradual weight loss during heating from 230 to 600 °C, corresponding to the removal of four DMF molecules (found 9.85%, calcd 8.53%). Then, during heating from 620 to 960 °C, the residual framework began to decompose, corresponding to the removal of the other DMF molecules and bibp ligands (found 17.29%, calcd 15.54%).

The cyclic voltammograms in 0.05 mol L^{-1} of H_2SO_4 are shown in Fig. 4. There are three pairs of reversible redox peaks (I–I′, II–II′, III–III′) in the potential range from + 0.1 to − 1.0 V, and the mean peak potentials $E_{1/2} = (E_{pa} + E_{pc})/2$ are − 0.28 V (I–I′), − 0.57 V (II–II′) and − 0.82 V (III–III′) at scan rate of 50 mV s^{-1}, The three pairs of reversible redox peaks are typical for the W-cluster which may be assigned to two one-electron and one two-electron wave (Teazea et al. 2007; Dong et al. 1995). Cd divalent transition metal cations do not exhibit electroactive at pH less than 3.

$$SiW_{12}^{VI}O_{40}^{4-} + e^- \leftrightarrow SiW^{V}W_{11}^{VI}O_{40}^{5-}(SiW_{12}O_{40}^{5-}) \quad (1)$$

$$SiW^{V}W_{11}^{VI}O_{40}^{5-} + e^- \leftrightarrow SiW_2^{V}W_{10}^{VI}O_{40}^{6-}(SiW_{12}O_{40}^{6-}) \quad (2)$$

$$SiW_2^{V}W_{10}^{VI}O_{40}^{6-} + 2e^- + 2H^+ \leftrightarrow H_2SiW_4^{V}W_8^{VI}O_{40}^{6-}(H_2SiW_{12}O_{40}^{6-}) \quad (3)$$

When the scan rate varied from 25 to 200 mV s^{-1}, the cathode and anode currents of peak increased, and the cathodic peak potentials shifted to the negative direction and the corresponding anodic peak potentials shifted to the positive direction. The anodic current of peaks (II) is proportional to the scan rates shown in the insets of Fig. 4, which suggests that the redox process is surface-control (Zonoz et al. 2014).

Figure 5 shows the cyclic voltammograms of **1** in the solution of 0.05 mol L^{-1} H_2SO_4 (A), and 0.05 mol L^{-1} $H_2SO_4 + 9.6\times10^{-3}$ mol L^{-1} $NaNO_2$ (B). Compared with the solution containing H_2SO_4, when the solution contains $NaNO_2$, the peak(II), and peak(III) are cannot be observed clearly, and a big and broad cathodic peak (IV′) is observed at − 0.38 V. The peak (IV′) would be assigned as nitrite reduction (Hao et al. 2012).

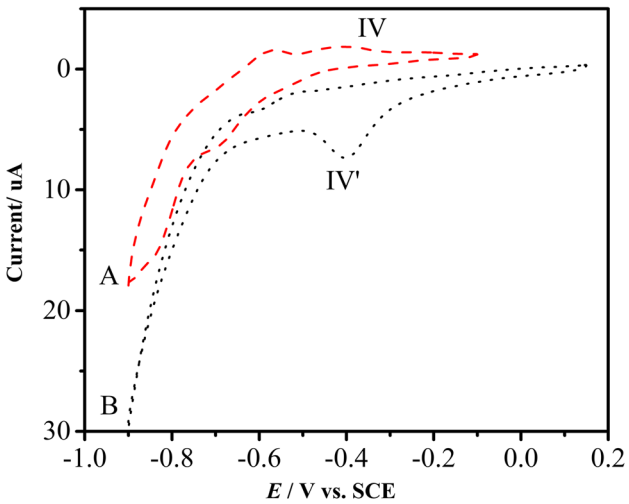

Fig. 5 Cyclic voltammograms of **1** in different solutions. (A) 0.05 mol L^{-1} H_2SO_4. (B) 0.05 mol L^{-1} $H_2SO_4 + 9.6\times10^{-3}$ mol L^{-1} $NaNO_2$. The scan rate was 50 mV s^{-1}

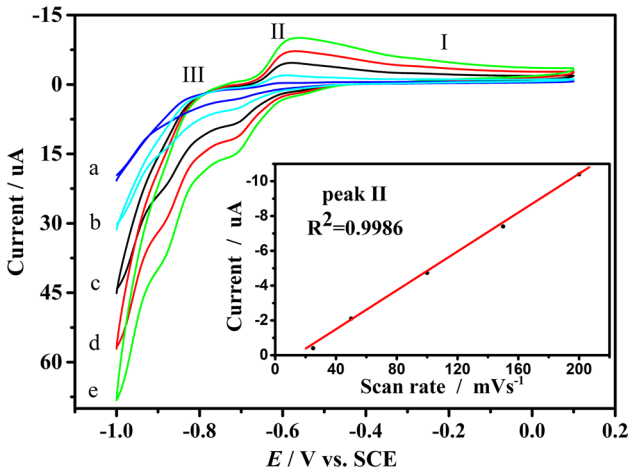

Fig. 4 Cyclic voltammograms of compound **1** in 0.05 mol L^{-1} H_2SO_4 solution at different scan rate (a 25, b 50, c 100, d 150, e 200 mV s^{-1}). The inset shows a plot of the anodic current of peak II against scan rate

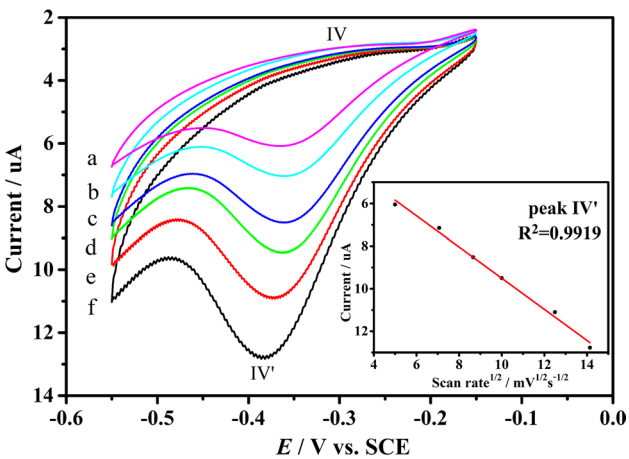

Fig. 6 Cyclic voltammograms of **1** in aqueous solution of 0.05 mol L^{-1} $H_2SO_4 + 9.6\times10^{-3}$ mol L^{-1} $NaNO_2$ at different scan rate (a 25, b 50, c 75, d 100, e 150, f 200 mV s^{-1}). The inset shows a plot of the anodic peak currents against the square root of the scan rate

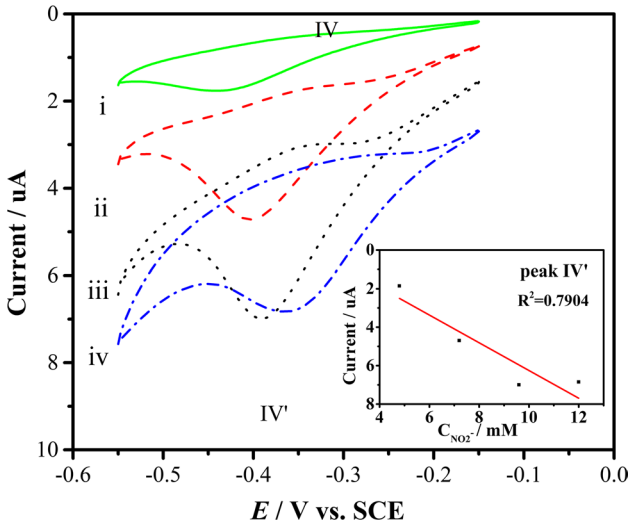

Fig. 7 Cyclic voltammograms (Scan rate 50 mV s^{-1}) of compound **1** in 0.05 mol L^{-1} $H_2SO_4 + NaNO_2$ solution, the concentration of $NaNO_2$: (i) 4.8×10^{-3} mol L^{-1}. (ii) 7.2×10^{-3} mol L^{-1}. (iii) 9.6×10^{-3} mol L^{-1}. (iv) 12.0×10^{-3} mol L^{-1}. The inset shows the relationship between cathode current and NO_2^- concentration

When the scan rate increased, the cathodic peak potentials shifted negatively, and the corresponding anodic peak potentials shifted positively (Fig. 6), The cathodic current of the peak (IV′) is proportional to the square root of the scan rate is shown in the inset of Fig. 6, as expected for a diffusion-controlled process. (Zonoz et al. 2014).

Figure 7 shows the cyclic voltammograms of **1** in the different concentration of the $NaNO_2$ solution. The electrocatalytic efficiency (abbreviate as CAT) are worked out by using the formula: $CAT = [I_p(POM, NaNO_2) - I_p(POM)] \times 100\%/I_p(POM)$, where $I_p(POM, NaNO_2)$ or $I_p(POM)$ is the cathodic peak currents in the solution with or without nitrite. The CAT of **1** was 1844.4%, which is bigger than the report of uncoordinated silicotungstic acid $H_4[SiW_{12}O_{40}] \cdot xH_2O$ (CAT, 470.7%) and $[Himi]_4[SiW_{12}O_{40}] \cdot H_2O$ (CAT, 600%) (Zonoz et al. 2013). It was indicated that the coordination environment had an effect on catalytic efficiency.

Conclusions

The new Keggin-type heteropolyoxometalates compound $\{[Cd(DMA)_4]_2(bibp)(SiW_{12}O_{40})\}_n$ (**1**) has been synthesized, purified, and characterized. In compound **1**, the $[SiW_{12}O_{40}]^{4-}$ anions and bibp ligands are linked by coordinated Cd^{2+} ions alternately into a zigzag-like chain, and the chains are extended into a 3D framework by the C–H···O hydrogen bonds. The cyclic voltammetry analyses show that compound **1** presences of W-centered reversible redox processes and that **1** has electrocatalytic activities towards the reduction of nitrite.

Acknowledgements This work was supported by the National Natural Science Foundation of China [Grant numbers 51672271]; the National Natural Science Foundation of China [Grant numbers 21701172]; the Key Project of Science and Technology Plan of Fujian Province [Grant numbers 2014H0007]; and the Fujian University of Technology [Grant numbers GY-Z12088].

Compliances with ethical standards

Conflict of interest On behalf of all authors, the corresponding author states that there is no.

References

Brese NE, O'keeffe M (1991) Bond-valence parameters for solids. Acta Crystallogr B 47:192–197. https://doi.org/10.1107/S0108768190011041

Dong S, Xi X, Tian M (1995) Study of the electrocatalytic reduction of nitrite with silicotungstic heteropolyanion. J Electroanal Chem 385:227–233. https://doi.org/10.1016/0022-0728(94)03770-4

Enferadi-Kerenkan A, Do TO, Kaliaguine S (2018) Heterogeneous catalysis by tungsten-based heteropoly compounds. Catal Sci Technol 8:2257–2284. https://doi.org/10.1039/c8cy00281a

Fan J, Hanson BE (2005) A two-dimensional cationic lattice built from $[Zn_6(HPO4)_2(PO4)_2]^{2+}$ clusters. Chem Commun 18:2327–2329. https://doi.org/10.1039/b501221j

Flack HD, Bernardinelli G (2000) Reporting and evaluating absolute-structure and absolute-configuration determinations. J Appl Cryst 33:1143–1148. https://doi.org/10.1107/S0021889800007184

Hao XL, Ma YY, Zhang C, Wang Q, Cheng X, Wang YH, Li YG, Wang EB (2012) Assembly of new organic-inorganic hybrids based on copper-bis (triazole) complexes and Keggin-type polyoxometalates with different negative charges. CrystEngComm 14:6573–6580. https://doi.org/10.1039/c2ce25747e

Hu SY, Ma CC, Zhan FY, Cao YL, Hu PF, Zhen Q (2017) Batch synthesis of polyoxometalate-based phosphonium compounds by one-step room-temperature mechanochemical process, and their morphology-dependent antibacterial activities. Chem Pap 71:1–7. https://doi.org/10.1007/s11696-016-0124-1

Jiang XY, Wu XY, Yu RM, Yuan DQ, Chen WZ (2011) A glycine ligand coordinated hybrid complex constructed from hexanuclear copper clusters and octamolybdates. Inorg Chem Commun 14:1546–1549. https://doi.org/10.1016/j.inoche.2011.05.001

Kong Z, Wang CL, Ren YH, Gu M, Hu YC, Yue B, He HY (2012) Synthesis, structure, and properties of two supramolecular compounds based on silicotungstic acid and transition metal (II) coordinated isonicotinic acid. Chin J Chem 30:759–764. https://doi.org/10.1002/cjoc.201100439

Meng XM, Zhang X, Qi PF, Zong ZA, Jin F, Fan YH (2017) Syntheses, structures, luminescent and photocatalytic properties of various polymers based on a "V"-shaped dicarboxylic acid. Rsc Adv 7:4855–4871. https://doi.org/10.1039/c6ra27509e

Proust A, Thouvenot R, Gouzerh P (2008) Functionalization of polyoxometalates: towards advanced applications in catalysis and materials science. Chem Commun 39:1837–1852. https://doi.org/10.1039/b715502f

Sheldrick GM (2015) Crystal structure refinement with SHELXL. Acta Crystallogr C 71:3–8. https://doi.org/10.1107/S2053229614024218

Shi ZY, Zhang ZY, Peng J, Yu X, Wang X (2013) Assembly of copper–tetrazole frameworks with role-changeable Keggin clusters: syntheses, structures, solvent-dependent luminescence and electrochemistry properties. CrystEngComm 15:7199–7205. https://doi.org/10.1039/c3ce41008k

Silva MJD, Oliveira CMD (2018) Catalysis by Keggin heteropolyacid salts. Curr Catal 7:26–34. https://doi.org/10.2174/2211544707666171219161414

Teazea A, Hervea G, Finke RG, Lyon DK (2007) α-, β-, and γ-dodecatungstosilicic acids: isomers and related lacunary compounds. Inorg Synth 27:85–96. https://doi.org/10.1002/9780470132586.ch16

Wu XY, Yang WB, Wu WM, Liao JZ, Wang SS, Lu CZ (2017) A inorganic-organic hybrid material constructed from the monolacunary polyoxomolybdates and multi-nuclear copper clusters. Inorg Chem Commun 76:118–121. https://doi.org/10.1016/j.inoche.2017.01.026

Zhang CL, Qin L, Zheng HG (2013) Synthesis, characterization and crystal structure of one Mn(II) complex with 4,4′-bisimidazolylbiphenyl and 4,4′-sulfonyldibenzoic acid. Inorg Chem Commun 34:34–36. https://doi.org/10.1016/j.inoche.2013.05.006

Zhao JW, Li YZ, Chen LJ, Yang GY (2016) Research progress on polyoxometalate-based transition-metal-rare-earth heterometallic derived materials: synthetic strategies, structural overview and functional applications. Chem Commun 52:4418–4445. https://doi.org/10.1039/c5cc10447e

Zhao WJ, Tan JT, Li X, Lu YL, Feng X, Yang XW (2014) Two new frameworks for biphenyl-3, 3′, 5, 5′-tetracarboxylic acid and nitrogen-containing organics. Chem Pap 68:1415–1420. https://doi.org/10.2478/s11696-014-0584-0

Zonoz FM, Jamshidi A, Tavakoli S (2013) Preparation, characterization and electrochemical investigation of a new inorganic-organic hybrid material based on keggin-type polyoxometalate and organic imidazole cation. Solid State Sci 17:83–89. https://doi.org/10.1016/j.solidstatesciences.2012.10.029

Zonoz FM, Zonoz IM, Jamshidi A, Alizadeh MH (2014) Synthesis, characterization and electrochemical investigation of a new inorganic-organic hybrid compound constructed by Keggin-type polyoxometalate and cyanoguanidine. Solid State Sci 32:13–19. https://doi.org/10.1016/j.solidstatesciences.2014.03.010

Publisher's Note Springer Nature remains neutral with regard to jurisdictional claims in published maps and institutional affiliations.